Volume 12, No 2 | International Journal of Radiation Research, April 2014

An investigation into the potential applicability of gel dosimeters for dosimetry in boron neutron capture therapy

S.M. Abtahi[1*], S.M.R. Aghamiri[1], H. Khalafi[2], F. Rahmani[1]

[1]University of Shahid Beheshti, Radiation Medicine Department, P. O. Box 19839- 63113, Tehran, Iran
[2]Nuclear Science and Technology Research Institute (NSTRI), Tehran, Iran

► *Original article*

**** Corresponding author:***
Dr. S.M. Abtahi,
Fax: *+98 21 22431780*
E-mail: *sm_abtahi@sbu.ac.ir*

Received: Oct. 2012
Accepted: July 2013

Int. J. Radiat. Res., April 2014; 12(2): 139-149

ABSTRACT

Background: The aim of this work was to establish how well gel dosimeters performed, as substitutes for brain tissue compared with standard phantom materials such as water, polymethyl-methacrylate (or PMMA), A150 plastic and TE- liquid phantom material for dosimetry of neutron beams in boron neutron capture therapy. ***Materials and Methods:*** Thermal neutron fluence, photon dose and epithermal neutron dose distributions were computed for the epithermal neutron beam of the optimized linac based BNCT. ***Results:*** Amongst all investigated phantom materials, TE-liquid was shown to be a better substitute for brain tissue than other phantom materials. The differences between TE- liquid and brain at the depth of 6.1 cm for thermal neutron fluence, gamma dose and epithermal neutron dose distributions was calculated 2.80%, 2.40% and -13.87% , respectively. In comparison with the other gel dosimeters, LMD2 provided a better simulation of radiation transport in the brain. It's results differed from the real brain, at the depth of 6.1 cm, for thermal neutron fluence, gamma dose and epithermal neutron dose distributions, by -1.27%, 4.20% and 21.05% respectively. C***onclusion:*** Even though, in gamma dose distribution the LMD2 has large deviation from brain tissue distribution, the deviation is approximately independent of depth, so the results can be multiplied by a constant coefficient to be more consistent with reality. Even though, TE- liquid showed satisfactory results for brain tissue substitution in BNCT, but some properties of gel dosimeters such as three dimensionality, make LMD2 a potentially good dosimeter for dosimetric verification in BNCT.

Keywords: *Gel dosimetry, BNCT, phantom, MCNP, dose distribution.*

INTRODUCTION

With a growing interest in the use of gel dosimeters for radiotherapy purposes, there is a need to address the question of ''what is the best gel dosimeter to use?''. This paper considers this question for Boron Neutron Capture Therapy (BNCT) by using Monte Carlo calculation by MCNP code. To this purpose flux and dose distribution in 17 gel dosimeters and some other materials of interest were investigated.

The main absorbed dose in BNCT, consists of the boron dose by the $^{10}B(n,\alpha)^{7}Li$ reaction, the nitrogen dose by the $^{14}N(n,p)^{14}C$, the hydrogen dose by the $^{1}H(n,n)^{1}H$, the gamma dose in patient's body by the $^{1}H(n,\gamma)^{2}H$, and the gamma dose produced due to neutron capture in the components of beam shaping assembly (BSA) and collimator. The boron dose and the nitrogen dose have the same spatial distribution as the thermal neutron fluence. The dose deposited due to proton recoils (or epithermal neutron

dose) depends on the incident neutron energy spectrum and has a similar spatial dependence to the epithermal neutron fluence [1] .

Many authors have investigated the water/ tissue equivalency of gel dosimeters for gamma irradiation [2-5] and some researchers investigated the use of some gel dosimeters for BNCT dosimetry [6-8]. But the question of " what is the best gel dosimeter for BNCT?" is still remained. The aim of this work was to establish how well, gel dosimeters would perform as substitutes for brain tissue compared with standard phantom materials such as water, polymethyl-methacrylate (or PMMA) and A150 plastic, for dosimetry of neutron beams for BNCT.

Gel dosimeters are fabricated from radiation sensitive materials which, upon irradiation, some of their characteristics change as a function of the absorbed radiation dose. In respect to these changes there are various methods for gel response reading [9]. Polymer gel dosimeters have several advantages such as high spatial resolution, feasibility of three-dimensional dosimetry [10] and they act as a phantom as well as a detector and do not require the use of perturbation correction factor [2]. However, this study does not investigate the agreement between doses derived from reading techniques and physical doses for such gels.

MATERIALS AND METHODS

Different types of materials, including some gel dosimeters and other standard phantom materials, were studied to evaluate whether they are tissue equivalent for neutron irradiation of BNCT technique or not. Here, in this work , the gel dosimeters were BANG-1 [11, 12], BANG-2 [13], BANG-3 [5, 14], VIPAR [15], PABIG [5], PAG [16], nPAG [16], nMAG [16], MAGIC [17], PAGAT [18, 19], MAGAS [4, 20], MAGAT [4], FGX [21], TGB [21], PERSAGE [3, 22], LMD1 and LMD2 [23]. These names were the acronyms due to the use of the chemical components mentioned in table 1. For example the acronym PAG was extracted from Gelatin, BIS and Acrylamide. In addition, flux and dose distributions in water, PMMA phantom material [1, 24], A150 [1] and Tissue Equivalent (TE)-liquid phantom materials [24], polyethylene (PE) [25], muscle [21, 26] and fat [18] were considered and all results were compared with brain tissue [1, 26].

Different chemical and elemental compositions of gel dosimeters are summarized in table 1 and table 2 respectively.

Monte Carlo simulations

The Monte Carlo code MCNP5 [27] was used to simulate the radiation transport generated by the 20 MeV linac-based epithermal neutron

Table 1. Different formulations published for normoxic polymer gel dosimeters.

gel dosimeters designations	Gel Dosimeter Formulation
PAG	Gelatin, BIS, acrylamide, water
nMAG	Methacrylic acid, Bis[tetrakis (hydroxymethyl) phosphonium]sulfate, gelatin
nPAG	Acryl amide, *N*,*N*-methylene-bis-acrylamide, Bis[tetrakis(hydroxymethyl) phosphonium] sulfate, gelatin
BANG-1	Acrylamide, N, N'-methylene-bisaclylamide cross-linker (bis), Gelatin, water
BANG-2	Bis, Acrylic acid, sodium hydroxide, Gelatin, water
BANG-3	Gelatin, N,N_-methylenebisacrylamide (MAA), water
VIPAR	N-Vinyl Pyrolidone Argon gel
PABIG	poly(ethylene glycol) diacrylate, *N*,*N*'-methylenebisacrylamide, gelatine, water
FXG	water, Phytagel, Potassium ferricyanide, Ferric chloride, Ferric ammonium citrate, Hydrochloric acid
TGB	Water, Gelatine, Ferrous ammonium sulphate, Xylenol, Sulphuric acid
PERSAGE	Polyurethane, radiochromic components (leuco dyes), halogen containing free radical initiators
LMD1	gelatin, a leucodye (LMG), trichloroacetic acid (CCl3COOH),Triton X-100, water
LMD2	gelatin, a leucodye (LMG), trichloroacetic acid (CCl3COOH), sodium dodecyl sulfate (SDS), water
MAGIC	Methacrylic acid, ascorbic acid, hydroquinone, CuSO4·5H2O,gelatin
MAGAS	Methacrylic acid, ascorbic acid, gelatin
MAGAT	Methacrylic acid, tetrakis (hydroxymethyl) phosphonium chloride, gelatin
PAGAT	Acrylamide, *N*,*N*-methylene-bis-acrylamide, tetrakis (hydroxymethyl) phosphonium chloride, hydroquinone, gelatin

Table 2. Elemental compositions of gel dosimeters and some materials of interest.

Media	Elemental composition (% by weight)											ρ(g/m^3)
	$_1$H	$_6$C	$_7$N	$_8$O	$_{11}$Na	$_{15}$P	$_{16}$S	$_{17}$Cl	$_{19}$K	$_5$B	others	
PAG	10.74	6.20	2.18	80.88	-	-	-	-	-	-	-	1.035
nMAG	10.68	7.45	1.39	80.43	-	0.03	0.02	-	-	-	-	1.046
nPAG	10.73	6.25	2.18	80.80	-	0.03	0.02	-	-	-	-	1.035
BANG-1	10.7	4.7	1.7	82.9	-	-	-	-	-	-	-	1.02
BANG-2	10.51	5.64	1.35	81.73	0.58	-	-	-	-	-	-	1.030
BANG-3	10.4	10.5	2.4	76.7	-	-	-	-	-	-	-	1.05
VIPAR	10.74	7.18	2.06	80.01	-	-	-	-	-	-	-	1.018
PABIG	10.75	6.78	1.56	80.91	-	-	-	-	-	-	-	1.02
FXG	11.0	2.5	0. 9	85.5	<0.1	-	0. 1	-	-	-	$_{26}$Fe <0.1	1.014
TGB	11.2	0. 2	<0.1	88.6	-	-	-	<0.1	<0.1	-	$_{26}$Fe <0.1	1.001
PERSAGE	8.92	60.74	4.46	21.72	-	-	-	3.34	-	-	$_{35}$Br 0. 84	1.101
LMD1	11.04	2.29	0.01	86.49	-	-	-	0.17	-	-	-	1.015
LMD2	10.87	3.79	0.01	84.14	0.16		0. 11	0.91				1.012
MAGIC	10.62	7.51	1.39	80.21	-	-	2.58×10^{-6}	-	-	-	$_{29}$Cu:5.08×10^{-6}	1.060
MAGAS	10.47	8.44	1.15	79.84	-	-	-	-	-	-	-	1038
MAGAT	10.42	8.54	1.15	79.28	-	0.15	-	0.17	-	-	-	1032
PAGAT	10.59	6.81	2.42	80.08	-	0.02		0.02	-	-	-	1.026
Water	11.19	-	-	88.81	-	-	-	-	-	-	-	1.00
Muscle	10.2	12.3	3.5	72.9	0.08	0. 2	0. 5	-	0. 3	-	$_{12}$Mg 0.02	1.040
Fat	11.20	57.32	1.10	30.31	-	-	6.0×10^{-3}	-	-	-	-	0.916
PMMA	8.0	60.0	-	32.0	-	-	-	-	-	-	-	1.190
A150	10.1	77.7	3.5	5.2	-	-	-	-	-	-	$_9$F 1.7,$_{20}$Ca 1.8	1.120
TE-liquid	10.2	12	3.6	74.2	-	-	-	-	-	-	-	1.070
Polyethylene	14.4	85.6	-	-	-	-	-	-	-	-	-	0.920
brain	10.7	14.5	2.2	71.2	0.2	0.4	0.2	0.3	0.3	-	-	1.040

beam. The source spectra reported in Rahmani and Shahriari [28] were used for this work. Epithermal (0.55 eV–10 keV) and fast (10 keV–10 MeV) neutrons, which are unavoidably present in the beam, interact mainly through the proton recoil process. The dose from this process will be referred, in this work, as the epithermal neutron dose. For clinical dosimetry purposes, three main dose components, i.e., thermal neutron fluence, gamma-ray dose and fast neutron dose, should be determined with a high accuracy under clinically relevant conditions.

The epithermal and thermal neutron fluxes, denoted by φ_{ep} and φ_t, respectively, were described with the following energy group subdivision for this study:

Epithermal group 0.55 eV ≤ E
Thermal group 0.55 eV > E

As shown in figure 1, the epithermal beam was directed into a Snyder head phantom [29, 30] filled with the various materials. Thermal neutron fluence, epithermal neutron dose and gamma dose distributions were calculated every 4 mm along the central axis of the head phantom. Gamma contamination of the source wasn't considered in this study and only gamma dose distribution resulted from neutron interaction with brain and it's substitute materials were considered. In other studies tissue equivalency of gel dosimeters in gamma irradiation have been investigated [2, 3]. The dose rate from epithermal neutrons and photons were derived using energy-dependent flux-to-dose conversion coefficients from track length estimates averaged over cubes (16 mm in length, 16 mm in wide, and 4 mm in height, height was along the beam axis). Kerma factors for brain tissue were used for both brain tissue and brain tissue substitutes [31]. Photon and neutron kerma factors are energy-dependent factors used to convert neutron or photon fluence spectra to kerma, which approximates absorbed dose.

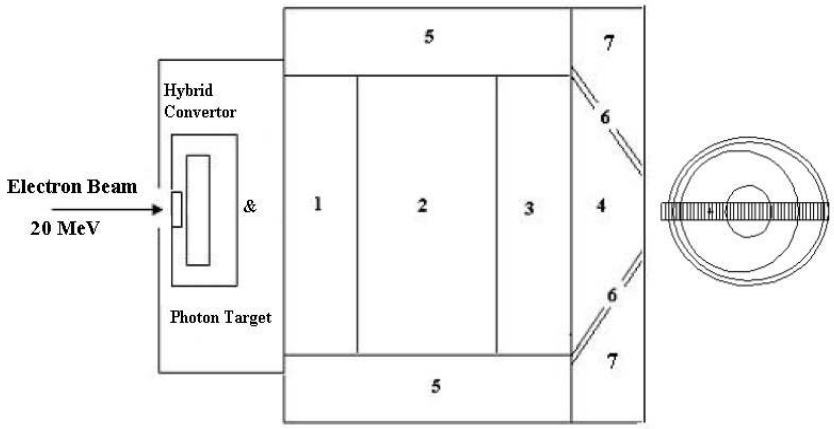

Figure 1. Beam shaping assembly used in the MCNP simulations. 1: Fe, 2: MgF_2, 3: CF_2, 4: Neutron path (cavity), 5: Pb, shield and reflector, 6: Ni collimator, 7: borated poly ethylene, neutron shield [28].

H, C, N, O and P kermas were based on kerma factors on ICRU 63 (ENDF/B-VI) and neutron kerma factors for Cl and S were based on JENDL 3.2 cross section data and reaction Q values. Photon kerma factors for brain tissue composition used in these calculations are based on mass energy absorption coefficients calculated by Seltzer [29].

In order to account the effect of the binding energy of individual nuclei on the interaction between thermal neutrons and the considered material, the free-gas treatment can be used down to the 4 eV. At this energy, the neutron energy is comparable to the thermal energy of the target atom as well as to its chemical binding energy. Molecular binding effects of hydrogen in different materials have been accounted. In the biological materials, some gels, TE-liquid and water, the thermal scattering treatment (S(α, β)) for hydrogen in light water, and for PERSAGE gel dosimeter, PMMA, A-150 tissue-equivalent plastic and polyethylene hydrogen in polyethylene was generally used.

Thermal neutron fluence, epithermal neutron dose and gamma dose distributions produced in the various phantom materials were compared. table 3 presents calculation results of absorbed dose at the maximum thermal neutron fluence in brain (1.3 cm) and at 6.1 cm depth. Each calculated distribution in the brain tissue was normalized to its own maximum value (figure 2).

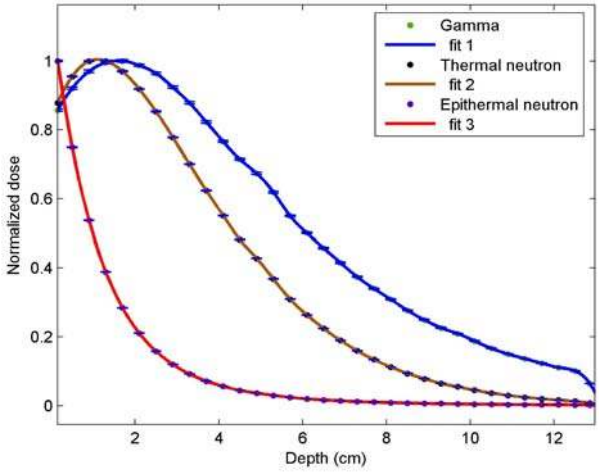

Figure 2. Normalized dose distribution of different radiation components.

RESULTS

Thermal neutron fluence distribution

Figure 3 shows the ratio of brain substitute to brain tissue for thermal neutron fluences. All MCNP5 calculations in all materials have relative errors less than 0.70%.

The best and worst performances were belong to LMD2 and polyethylene respectively. Maximum and minimum deviations from brain tissue at the deepest calculation point are 83% and 0%, respectively. Except PERSAGE, all other gel dosimeters showed generally better performance than water. TE-liquid phantom material showed the best performance from entrance

point up to 4.5 cm, but in deeper positions the LMD-2 showed the best performance. Among the gel dosimeters, PERSAGE showed the worst responses with -15.5% to -47.5% deviations at 0.15 and 12.1 cm in depth, respectively. Except PERSAGE, maximum difference between 10%-27.3% has been observed for MAGIC, MAGAS and MAGAT respectively, at the deepest or near deepest calculation point. In non gel phantoms, except TE - liquid, A150 plastic also had an acceptable behavior close to 4 cm depth. At this point brain and A150 plastic had the same results. Deviation increased in point located before and after this point (figure 3).

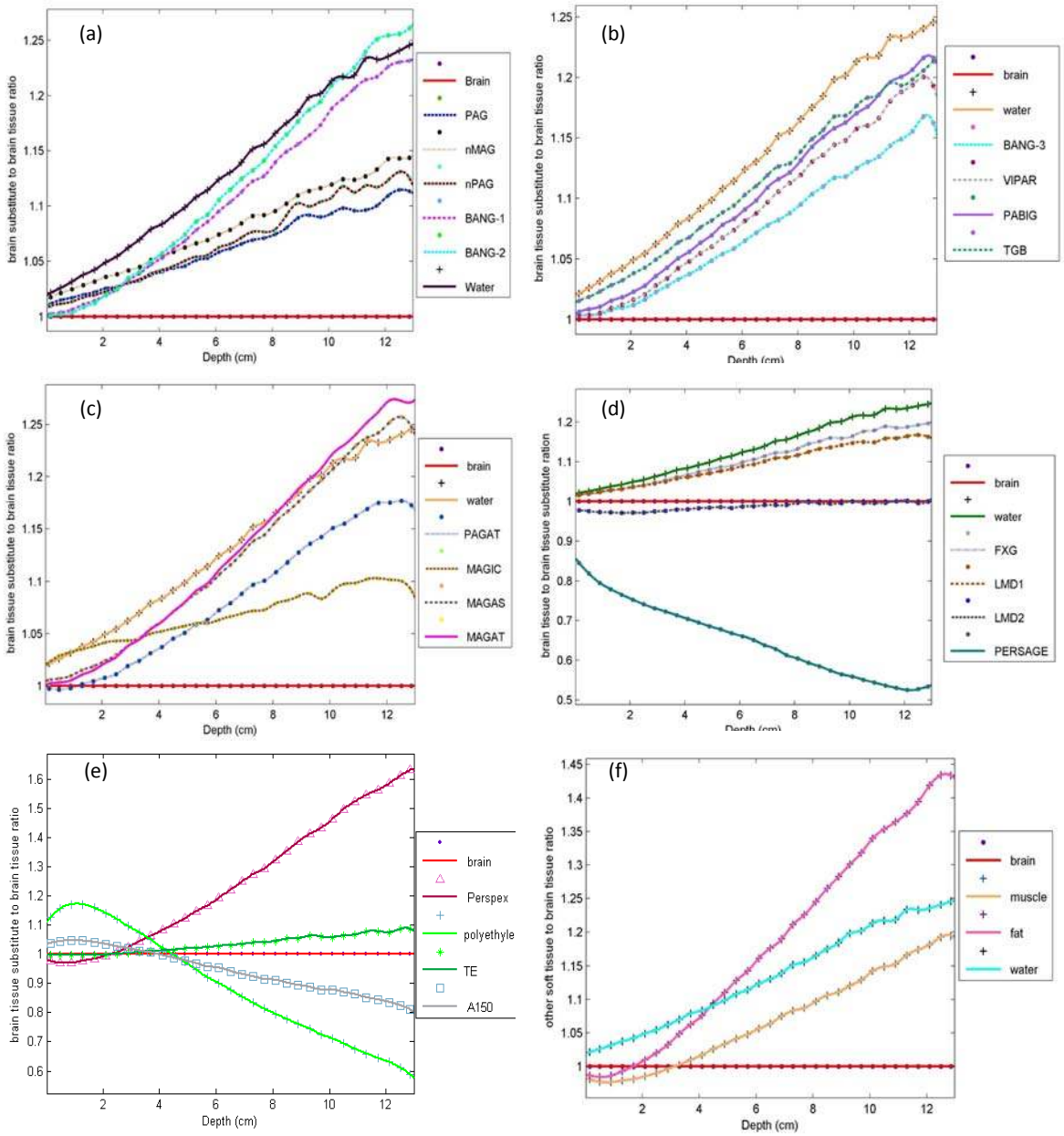

Figure 3. Thermal neutron fluence distribution in tissue substitute to brain tissue ratio for a) PAG, nMAG, nPAG, BANG-1 and BANG-2, b) BANG-3, VIPAR, PABIG and TGB, c) PAGAT, MAGIC, MAGAS and MAGAT, d) FXG, LMD1, LMD2 and PERSAGE, e) polyethylene, A150, TE-liquid tissue equivalent and Perspex and f) other soft tissues include fat and muscle. In all cases, fluence distribution in water phantom is shown.

Epithermal neutron dose distribution

As stated in section 2.1, neutrons with energy above 0.5 eV was named epithermal neutrons. Figure 4 shows epithermal neutron dose in tissue substitute materials normalized to brain tissue. nMAG gel dosimeter has the best performance for epithermal neutron dose distribution which has maximum deference about -0.4% from brain tissue at 7.7 cm in depth. Subsequent choices based on epithermal neutron dose criterion are PAG and LMD1, respectively. In gel dosimeters, the PERSAGE had the worst response with 15% in maximum deviation from brain tissue at depth of 7.3 cm. In non gel phantoms, TE- liquid showed adequate tissue equivalency with maximum deviation of -2.6% from brain at depth of 5.7 cm. Other gels showed maximum deviation from brain distribution from 2% for nPAG to 6.6% for BANG-2, at the near deepest calculation point. The uncertainties of all Monte Carlo calculations were less than 0.70% (1SD).

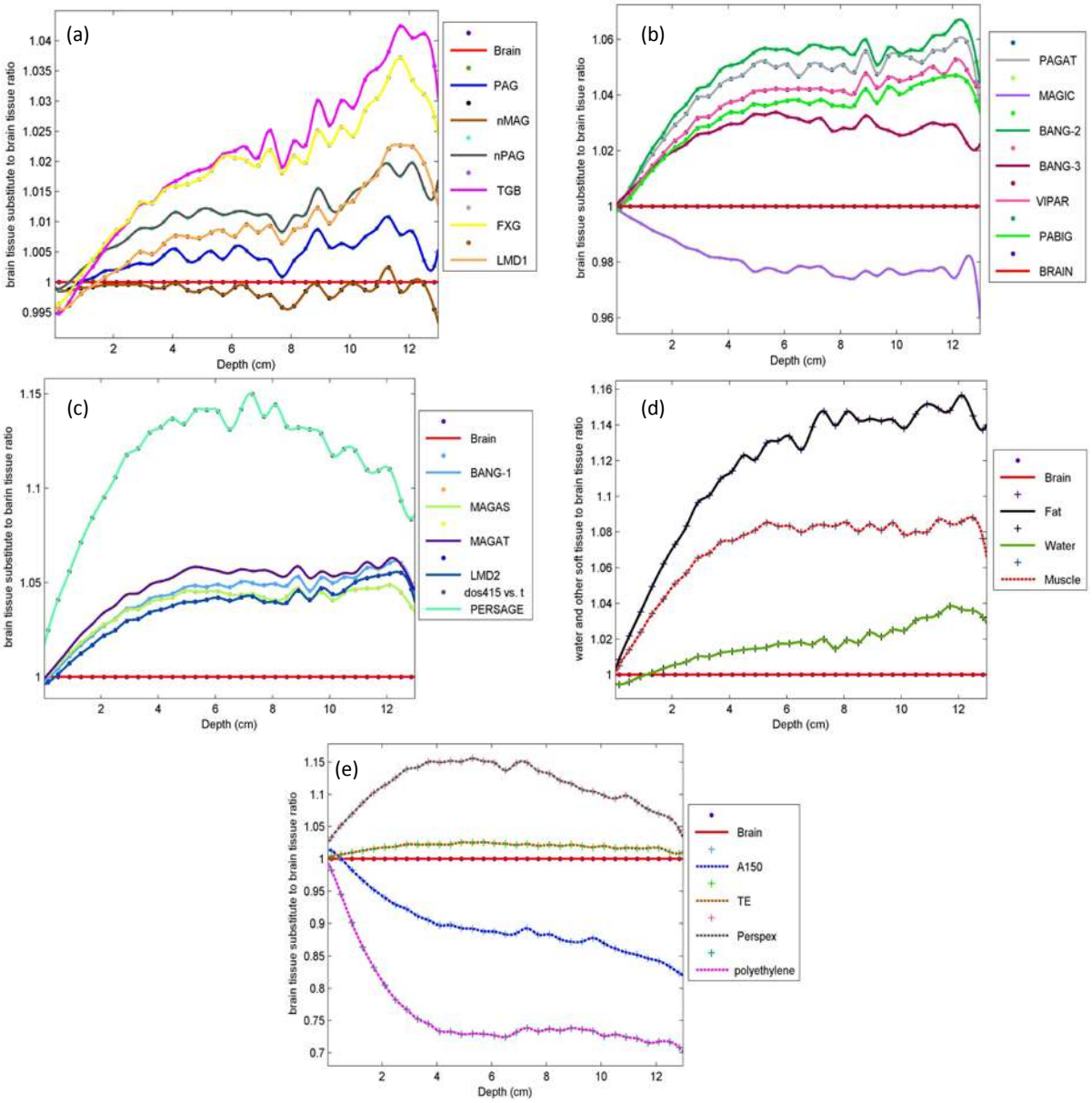

Figure 4. Epithermal neutron dose of brain tissue substitutes normalized to brain tissue.

Gamma dose distribution

Figure 5 shows the gamma doses in brain substitute which were normalized to those in brain tissue. Amongst all investigated materials, the LMD1 and TGB gel dosimeters had satisfactory results with maximum deviations of −4.7% and −7.2%, respectively. In non gel phantoms, polyethylene and water provide the best response with the maximum difference of 10.7% and 10.8% compared to brain tissue, respectively.

Again, PERSAGE gel dosimeter showed the largest deviation with a difference of −70.2% at a depth of 1.7 cm. The next material with large deviation was PMMA with difference of -25.5% at depth of 2.1 cm .The uncertainties of all calculations were less than 0.73% (1SD).

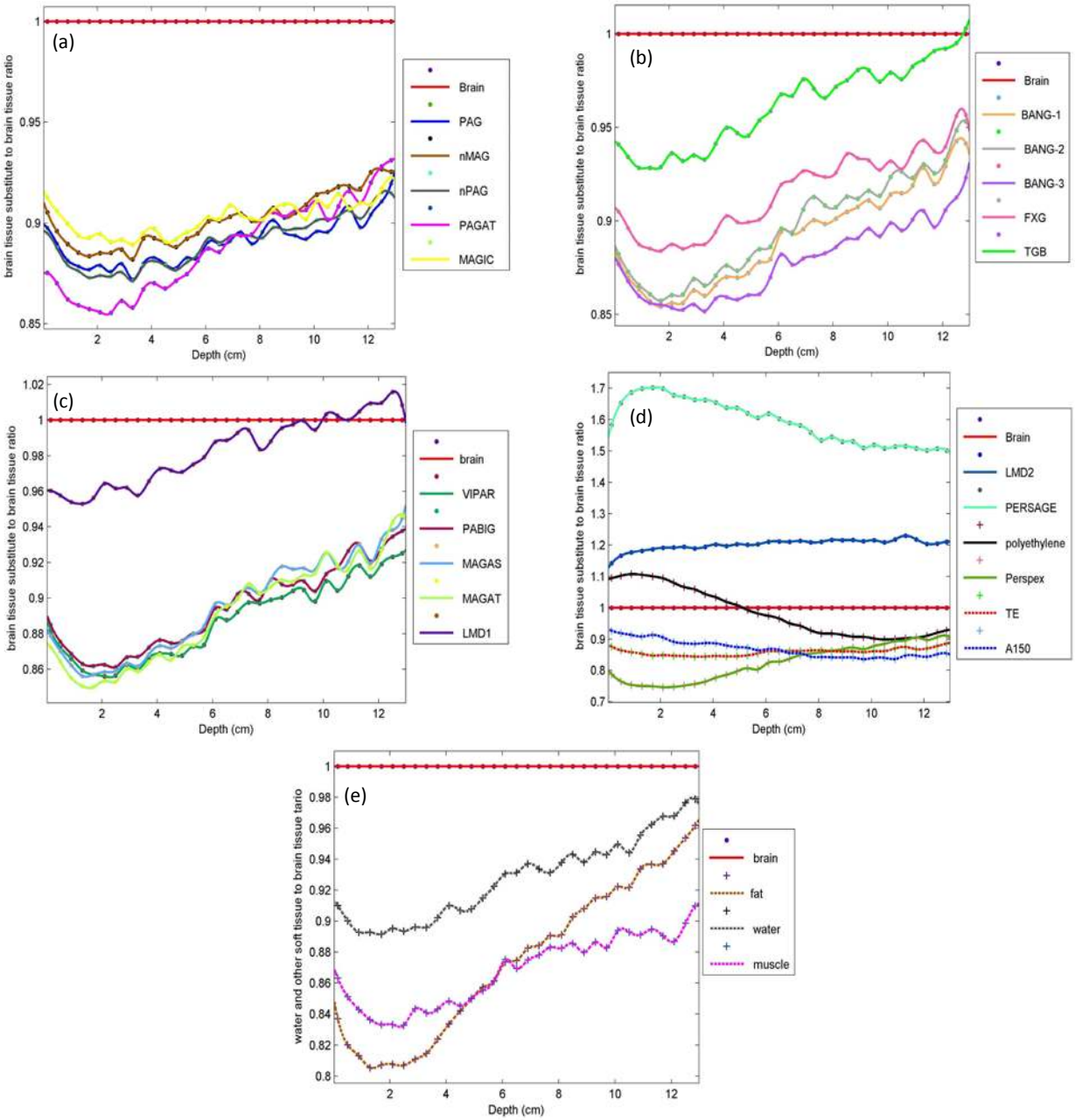

Figure 5. Gamma dose in brain tissue substitutes normalized to brain tissue.

Table 3. Differences of thermal neutron fluence, epithermal neutron and photon doses relative to the brain tissue at the depth of maximum thermal neutron fluence and at 6.1 cm in depth

	Thermal neutron (%)		Epithermal neutron (%)		Gamma (%)	
Material	1.3 cm	6.1 cm	1.3 cm	6.1 cm	1.3 cm	6.1 cm
PAG	1.98	5.8271	0.0686	0.5852	-12.1518	-10.9235
nMAG	2.85	7.4094	-0.0801	-0.0835	-11.4588	-9.9095
nPAG	1.73	6.2510	0.3602	1.1651	-12.3870	-10.7409
PAGAT	0.16	7.2512	1.8795	5.0946	-14.0865	-11.2595
MAGIC	3.52	6.3048	-0.8602	-2.3720	-10.6173	-9.6970
BANG-1	1.09	9.5137	1.6919	4.8965	-14.2941	-10.5764
BANG-2	0.84	10.5456	2.0952	5.6343	-13.9176	-10.4136
BANG-3	0.77	6.5137	1.3841	3.2244	-14.3886	-11.7952
VIPAR	0.93	8.1466	1.4708	4.1929	-14.0645	-11.1903
PABIG	1.54	9.0981	1.3055	3.7936	-13.6960	-10.5584
TGB	2.83	10.3119	0.2589	2.1746	-7.1627	-3.2255
FXG	2.74	9.8925	0.3748	2.0585	-11.4779	-8.0620
MAGAS	1.50	10.6280	1.8136	4.5375	-14.3807	-10.3074
MAGAT	1.07	11.0886	2.2389	5.6115	-14.9482	-10.9549
PERSAGE	-22.12	-33.9523	7.1301	14.0793	69.9651	61.9221
LMD1	2.88	8.9101	-0.0609	0.7575	-4.6980	-1.2206
LMD2	-2.72	-1.2685	1.2377	4.1982	18.1914	21.0478
Fat	-0.71	16.1627	4.9359	13.3589	-19.4644	-12.6330
Water	3.77	12.3882	0.1125	1.7458	-10.7198	-6.9369
Muscle	-2.10	5.6388	3.4208	8.3380	-16.3594	-12.4871
A150	4.58	-4.6030	-3.3584	-11.2139	-9.2041	-13.1968
TE	-0.11	2.8041	1.2766	2.3978	-14.7243	-13.8663
Perspex	-2.24	19.4975	8.7115	14.9104	-24.9510	-17.5466
polyethylene	17.06	-9.8942	-13.6500	-27.3184	10.4968	-2.6079

DISCUSSION

Different gel dosimeters and non- gel phantom materials were investigated. With respect to simulated materials, in order to account molecular binding effects, thermal scattering treatment (S(α, β)) of hydrogen in light water and polyethylene were considered.

Neutron distribution in hydrogen enriched materials, irradiated with epithermal neutrons, are mainly determined by the hydrogen density of the phantom [24]. Carbon and oxygen can compensate the difference of hydrogen density. Although the cross sections of ^{37}Cl, ^{31}P and ^{39}K show some resonances [32], but the low percentages of these elements in comparison to hydrogen and also their heaviness against neutron can cause less neutron energy transfer to these elements. Therefore the effective elements for neutron thermalization are ^{1}H, ^{12}C, ^{14}N and ^{16}O.

^{1}H, ^{39}K, ^{37}Cl, ^{14}N and ^{31}P show relatively high absorption cross sections. ^{39}K and ^{37}Cl show resonance regions for epithermal neutrons absorption [32]. The difference between neutron absorption in these elements causes differences in gamma dose distributions.

TE- liquid phantom material showed satisfactory results for thermal neutron fluence distribution up to 4.5 cm in depth, while, for deeper than 4.5 cm, LMD2 gel dosimeter showed better results .

On the other hand in thermal neutron fluence distribution calculation, the TE- liquid phantom material showed better compatibility with the brain tissue compared to LMD2 up to 4.5 cm in depth, however some characteristics of LMD2 dosimeter [23], such as capability in 3D dosimetry, makes it more suitable than others in thermal neutron fluence distribution.

Since the hydrogen densities of LMD2, TE liquid and brain differ only a few percent (table

1), so minor differences have been observed between these materials in neutron transportation. The hydrogen density of polyethylene is significantly higher (34%) than that of brain, which explains higher absolute thermal neutron fluence and decreased penetration of thermal neutrons in polyethylene. Hydrogen scatters epithermal neutrons to lower energy by relatively high cross section (~20 barn). Carbon scatters neutrons with a cross section of about 5b in epithermal region [32]. Therefore fluence of thermal neutrons in shallow depths was increased with depth. In a distinguished depth, absorption of thermal neutrons will dominate over its scattering. Beyond this depth, thermal neutron fluence decreased.

Neutrons with energies more than 0.5ev interact with the studied materials mainly through the proton recoil process. Here, the dose of this process will be referred to as the epithermal neutron dose. Most of the phantom materials showed better agreement with brain tissue in epithermal neutron dose than the other dose components. Maximum deviation from brain tissue dose distribution belonged to PMMA, while the nMAG gel dosimeter had the best performance relative to brain tissue dose distribution, however PAG and LMD1 gel dosimeters also showed acceptable results. In non- gel phantom materials, TE- liquid showed good performance in epithermal neutron dose distribution. In other cases, gel dosimeters performed better as the brain tissue substitute than non-gel phantom materials in epithermal neutron dose distribution.

Epithermal neutron dose distribution in gel dosimeters encounters the drawback of LET dependence [33]. Epithermal neutrons produce a wide energy range of protons which consequently include a wide range of LETs. These protons induce different responses in gel dosimeter which integrated response is depends on proton's LETs. This makes it difficult to calibrate the gel dosimeter. Dose rate dependence in LMD1 and LMD2 gel dosimeters is another issue [23]. This means that more research is necessary to investigate the LET and dose rate dependence of some gel dosimeters such as LMD1, LMD2 and nMAG to further minimize the LET and dose rate dependence through optimization of gel formulation.

Here, in this work, gamma dose has been considered as a result of neutron capture in brain, gel dosimeters and phantom materials. For a better compatibility of gamma dose distribution between brain and its substitute materials, it is necessary to have the same neutron absorption cross section. Furthermore transport of the produced gamma in brain substitute materials and brain tissue should have similar behavior. This means that brain and brain substitute materials should have similar photoelectric and Compton scattering cross sections.

Amongst all investigated materials , the LMD1 and TGB gel dosimeters showed promising results for gamma dose distribution with a maximum deviation of −4.7% and −7.2% respectively from brain tissue values.

Results of this work is consistent with the results of Wojnecki and Green [1] in their study on investigation of 4 phantom materials as brain tissue substitutes for BNCT where it was stated that polyacrylamide gel and A-150 plastic performed well as brain tissue substitutes compared to PMMA and water. However, in this work 17 gel dosimeters and 5 non- gel phantom materials were simulated. Results showed that LMD2 and TE- liquid phantom material have a better performance compared to PAG gel dosimeter in thermal neutron fluence distribution. Among investigated materials, TE-liquid showed satisfactory results and were consistent with experimental investigation of Raaijmakers *et al.* [24] on water and 3 other phantom materials for BNCT. They compared absolute dose value and PDD curves for the various dose components of BNCT beams in water, PMMA, TE liquid and polyethylene. They observed minor differences, within approximately 4%, between absolute dose values at 2 cm depth in water and TE liquid. Our results are in accordance with their investigation too.

Raaijmakers *et al.* [24] reported values of higher differences in dose and fluence between water and polyethylene (PE). They showed that in PE, thermal neutron fluence, was

approximately 17% higher than in water. This finding agrees with our results that showed 10% higher thermal neutron fluence in the same depth for PE. According to their findings, the gamma dose, was approximately 34% higher at the depth of 2 cm in PE compared to water, while in our theoretical study 21.2% difference had been observed at a depth of 1.3 cm. Discrepancy between Raaijmakers et al. experiment and our theoretical results could have three different reasons. 1: different reference depths which were 2 and 1.3 cm in these two works, 2: different geometries of phantom and irradiation, 3: different spectrum of neutron beams, however this could be ignored [24]. Another experimental investigation by Jouni Uusi-Simola *et al.* [6], was performed on MAGIC polymer gel for dosimetric verification in BNCT. Our findings ,from cross sectional point of view, showed that innovation of LMD2 gel dosimeter [23], is more reliable for dose verification in BNCT. The deviations of thermal neutron fluence as the main component in BNCT for MAGIC polymer gel was calculated 3.52% and 6.30% in 1.3 and 6.1 depth respectively while this deviations reduced to 2.72% and 1.27% for LMD2 gel dosimeter. However, as shown in table 3 for other dose component, MAGIC performed better than LMD2.

With exception of TE- liquid, in non- gel phantom materials, and PERSAGE gel dosimeter, in gel phantom materials, generally other gel phantoms had better performance as a brain tissue substitute in dose verification of BNCT. LMD2, TE- liquid phantom material and PAG had three closer thermal dose distribution to that of brain, tissue respectively. For epithermal neutron dose distribution, nMAG, PAG and LMD1 showed closer results to that of brain respectively. However in epithermal neutron dose distribution, other gel dosimeters, water and TE-liquid by maximum deviation of 6.6% from brain tissue dose distribution, showed acceptable results. For gamma dose distribution, LMD1, TGB and water showed closer results to brain tissue dose distribution, respectively. Since thermal neutron is the most important radiation component in BNCT, LMD2 is recommended for BNCT dose verification. As shown in figure 4c, this gel dosimeter has a good behavior in epithermal dose distribution simulation. Even though, in gamma dose distribution, the LMD2 has a large deviation from brain tissue distribution, which is approximately independent of depth, therefore the results can multiplied by a constant factor to make it more consistent with reality.

CONCLUSION

Even though, TE- liquid is usually used as a brain tissue substitution in BNCT, some properties of gel dosimeters such as three dimensionality, sameness of detector and phantom as well as other interesting features of gel dosimeters make them a potentially good phantom- dosimeter for dosimetric verification in BNCT. According to our work, LMD2 can be used as a good phantom- dosimeter in BNCT. However more researches are required to investigate neutron energy dependence of LMD2 and further reduction of dose rate dependence and other inaccuracy sources of this gel dosimeter, through gel formulation and reading technique optimizations.

ACKNOWLEDGMENT

Useful discussions with Dr. Mohammad Hassan Zahmatkesh are highly appreciated. We also thank Dr. Abd al-hamid Minoochehr for useful discussions.

REFERENCES

1. Wojnecki C and Green S (2001) A computational study into the use of polyacrylamide gel and A-150 plastic as brain tissue substitutes for boron neutron capture therapy. *Phys Med Biol, **46**:1399–1405.*
2. Sellakumar P, Samuel EJJ, Supe SS (2007) Water equivalence of polymer gel dosimeters. *Radiation Physics and Chemistry, **76**: 1108-1115.*
3. Brown S, Venning A, Deene YD, Vial P, Oliver L, Adamovics J, *et al.* (2008) Radiological properties of the PRESAGE and PAGAT polymer dosimeters. *Applied Radiation and Isotopes,*

66:1970– 1974.
4. Venning AJ, Nitschke KN, Keall PJ, Baldock C (2005) Radiological properties of normoxic polymer gel dosimeters. *Medical Physics,* **32**(4):1047-53.
5. Pantelis E, Karlis AK, Kozicki M, Papagiannis P, Sakelliou L, Rosiak JM (2004) Polymer gel water equivalence and relative energy response with emphasis on low photon energy dosimetry in brachytherapy. *Physics in Medicine and Biology,* **49**: 3495-3514.
6. UusiSimola J, Heikkinen S, Kotiluoto P, Serén T, Seppälä T, Auterinen I, *et al.* (2007) MAGIC polymer gel for dosimetric verification in boron neutron capture therapy. J*ournal of Applied Clinical Medical Physics,* **8(2):** 114-123.
7. Uusi-Simola J, Savolainen S, Kangasm¨aki A, Heikkinen S (2003) Study of the relative dose-response of BANG-3R polymer gel dosimeters in epithermal neutron irradiation. *Phys Med Bio,* **48**: 2895–2906.
8. Farajollahi AR, Bonnett DE, Tattam D, Greenk S (2000) The potential use of polymer gel dosimetry in boron neutron capture therapy. *Phys Med Biol,* **45**: N9–N14.
9. Baldock C, Deene YD, Doran S, Ibbott G, Jirasek A, Lepage M, *et al.* (2010) Polymer gel dosimetry. *Phys Med Biol,* **55**:R1–R63.
10. Ibbott GS (2004) Application of gel dosimetry. *Journal of Physics,* **Conference Series 3**: 58-77.
11. Maryanski MJ, Schulz RJ, Ibbott GS, Gatenby JC, Xie J, Horton D, *et al.* (1994) Magnetic resonance imaging of radiation dose distributions using a polymer-gel dosimeter. *Physics in Medicine and Biology,* **39**:1437-1455.
12. Marya˜nski MJ, Zastavker YZ, Gore JC (1996) Radiation dose distributions in three dimensions from tomographic optical density scanning of polymer gels: II. Optical properties of the BANG polymer gel. *Phys Med Biol,* **41**:2705–2717.
13. Maryanski MJ, Ibbott GS, Eastman P, Scultz RJ, Gore JC (1996) Radiation therapy dosimetry using magnetic resonance imaging of polymer gels. *Med Phys,* **23**:699–705.
14. Bruce P (2003) The use of BANG-3 polymer gel to quantify the three-dimensional dose distribution of IMRT. [MSc. Thesis]. Louisiana: Louisiana State University, 27-28.
15. Pappas E, Maris T, Angelopoulos A, Paparigopoulou M, Sakelliou L, Sandilos P, *et al.* (1999) A new polymer gel for magnetic resonance imaging (MRI) radiation dosimetry. *Phys Med Biol,* **44**: 2677–2684.
16. Deene YD, Vergote K, Claeys C, Wagter Cd (2006) The fundamental radiation propertiesof normoxic polymer gel dosimeters: a comparison between a methacrylic acid based gel and acrylamide based gels. *Phys Med Biol,* **51**: 653 -673.
17. Fong PM, Keil DC, Does MD, Gore JC (2001) Polymer gels for magnetic resonance imaging of radiation dose distributions at normal room atmosphere. *Physics in Medicine and Biology,* **46**(12):3105-3113.
18. Venning AJ, Hill B, Brindha S, Healy BJ, Baldock C (2005) Investigation of the PAGAT polymer gel dosimeter using magnetic resonance imaging. *Physics in Medicine and Biology Printed in the UK,* **50**: 3875-3888.
19. Venning AJ, Brindha S, Hill B, Baldock C (2004) Preliminary study of a normoxic PAG gel dosimeter with tetrakis (hydroxymethyl) phosphonium chloride as an antioxidant. *Journal of Physics,* **Conference Series 3**: 155–158.
20. Venning A, Healy B, Nitschk K, Baldock C (2005) Investigation of the MAGAS normoxic polymer gel dosimeter with Pyrex glass walls for clinical radiotherapy dosimetry. *Nuclear Instruments and Methods in Physics Research A,* **555**(1-2): 396-402.
21. Šolc J and Sp˘ev´a˘cek Va (2009) New radiochromic gel for 3D dosimetry based on Turnbull blue: basic properties. *Phys Med Biol,* **54**: 5095–5107.
22. Gorjiara T, Hill R, Kuncic Z, Adamovics J, Bosi S, Kim J-H, *et al.* (2011) Investigation of radiological properties and water equivalency of PRESAGE® dosimeters. *Med Phys,* **38 (4)**
23. Vandecasteele J, Ghysel S, Baete SH, Deene YD (2011) Radio-physical properties of micelle leucodye 3D integrating gel dosimeters. *Phys Med Biol,* **56**: 627–651.
24. Raaijmakers CPJ, Nottelman EL, Mijnheer BJ (2000) Phantom materials for boron neutron capture therapy. *Phys Med Biol,* **45**:2353–2361.
25. Taylor ML, Franich RD, Johnston PN, Millar RM, Trapp JV (2007) Systematic variations in polymer gel dosimeter calibration due to container influence and deviations from water equivalence. *Phys Med Biol,* **52**: 3991–4005.
26. ICRU (1989) Tissue substitutes in radiation dosimetry and measurement. *Report No.: ICRU Report 44 (Bethesda, MD: ICRU).*
27. X-5 Monte Carlo Team. MCNP—A General Monte Carlo N-Particle Transport Code, Version 5, Volume I: Overview and Theory. Los Alamos, N.M.: Los Alamos National Laboratory; 2003. Report No.: LA-UR-03-1987.
28. Rahmani Fand Shahriari M (2011) Beam shaping assembly optimization of Linac based BNCT and in-phantom depth dose distribution analysis of brain tumors for verification of a beam model. *Annals of Nuclear Energy,* **38**: 404–409.
29. Goorley JT, Kiger WS, Zamenhof RG (2002) Reference dosimetry calculations for neutron capture therapy with comparison of analytical and voxel models. *Med Phys,* **29(2):** 145-156
30. Goorley JT (2007) MCNP Medical Physics Database: *Los Alamos National Laboratory, Report No.: LA-UR-07-2777.*
31. ICRU63 (2000) Nuclear data for neutron and proton radiotherapy and for radiation protection. MD Bethesda: *International Commission on Radiation Units and Measurements, 63.*
32. Nuclear Energy Agency (NEA) (2010). *JANIS-3.2. In Hauts-de-Seine,*
33. Gustavsson H, Ba¨ck SAJ, Medin J, Grusell E, Olsson LE (2004) Linear energy transfer dependence of a normoxic polymer gel dosimeter investigated using proton beam absorbed dose measurements. *Phys Med Biol,* **49**:3847–3855.